ELSEVIER

Materials Science and Engineering A344 (2003) 140–145

MATERIALS SCIENCE & ENGINEERING A

www.elsevier.com/locate/msea

Modelling the effective elasto-plastic properties of unidirectional composites reinforced by fibre bundles under transverse tension and shear loading

Qing-Sheng Yang [a], Qing-Hua Qin [b,c,*]

[a] Numerical Simulation Centre for Engineering, Department of Mechanics, Beijing Polytechnic University, Beijing 100022, PR China
[b] Department of Mechanics, Tianjin University, Tianjin 300072, PR China
[c] School of AMME, University of Sydney, Sydney, NSW 2006, Australia

Received 30 April 2001; received in revised form 23 May 2002

Abstract

The effect of fibre bundling on the effective transverse properties of unidirectional fibre composites has been investigated by way of finite element method and micromechanics models of fibre bundles. Based on the micromechanical model of single-fibre composites, plane strain models for composites reinforced by fibre bundles are presented. The effective elasto-plastic stress–strain behaviour was obtained numerically by analysing a boron/aluminium composite reinforced by three-fibre and four-fibre bundles. The results are compared with the modelled behaviour for the composites reinforced by single fibres. The study shows that there is a remarkable influence of fibre bundling on plastic deformation, transverse tension and shear tangent stiffness of composites, while the influence on effective elastic properties can be ignored, fibre bundling enhances the transverse tangent stiffness of plastic deformation of composite materials, and the transverse normal stress–strain relations are more sensitive to fibre bundling than the transverse shear stress–strain relations.

Keywords: Composites; Fibre bundling; Effective properties; Elasto-plasticity; Micromechanics

1. Introduction

Because of inhomogeneity and uneven distribution, there exist fibre-rich zones and matrix-rich zones in most practical fibre composites. This means that a fibre may be in contact with others within fibre-rich zones, while a fibre may be isolated within matrix-rich zones. Further, fibre-free zones could prevail in certain composites. For example, fibres in polymer–matrix composites may cluster locally as the matrix flows in the process of lamination and solidification even if the distribution of fibres is uniform in the single-layer slab [1]. Similarly, non-uniformity of fibre distribution also exists in metal–matrix and ceramic–matrix composites. Therefore, local clustering or bundling of fibres in composites (Fig. 1(a)) is common in practical engineering, and the modelling of fibre bundles seems to be an efficient tool for analysing such composites as discussed above. Thus, fibre bundling modelling of fibre composites has been the subject of much interest during the last decade [2–8], but modelling the effective material properties of fibre composites due to non-uniform distribution of fibres and determine the effect of fibre bundles on the composite performance still remain challenging tasks [4,6].

Fibre composites have usually been simplified as composites reinforced by isolated or uniformly distributed fibres in most previous theoretical analyses. These simplified composites can be referred to as single-fibre composites, as shown in Fig. 1(b). However, research has shown that uneven distribution of fibres can dramatically influence local stresses, thermally-induced residual stresses, and cracking behaviour of composites [9,10]. Therefore fibre bundling models (Fig. 1(c)) have been introduced in order to model the composites more

* Corresponding author. Tel.: +61-2-9351-7144; fax: +61-2-9351-3760
E-mail address: qin@mech.eng.usyd.edu.au (Q.-H. Qin).

0921-5093/02/$ - see front matter
PII: S0921-5093(02)00399-4

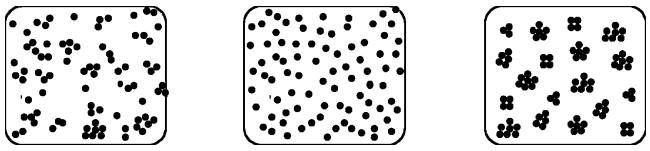

Fig. 1. Schemata of microstructure of fibre composites. (a) Real composite; (b) single-fibre composite; (c) fibre-bundle composite.

accurately. An important distinction between single-fibre and fibre-bundle reinforced composites is that marked fibre interaction and contact prevail in the latter. Tests were devised for failure analysis of fibre-bundle reinforced composites early in 1972 [11]. Fracture behaviour of fibre-bundle reinforced composites was investigated in Ref. [12]. Since that time, two mesostructure models, of orientation and packing mesostructures, have been advanced [1,13]. Typical examples of the two mesostructures are waviness of fibre and fibre bundling. The aforementioned studies [1,11] indicated that mesostructures of the composite can affect the ultimate properties and be influenced by the manufacturing process. However, there is still a lack of critical knowledge of the application of fibre bundling models to micromechanical analysis. This work deals with the micromechanical modelling and prediction of the effective transverse properties of unidirectional fibre-bundle reinforced composites. Both three-fibre and four-fibre bundle models are considered, to study the effect of fibre bundling on the effective mechanical properties of the fibre composites. The single-fibre model is used for comparison. Numerical examples of B/Al composites are considered, using transverse normal and shear elasto-plastic stress–strain relations.

2. Micromechanical modelling of fibre composites

2.1. Single-fibre model

In the single-fibre micromechanical model, uniform distribution of fibres in the matrix is assumed. Fig. 2 shows a typical single-fibre micromechanical model. Obviously this is an idealization of the microstructure of fibre composites. Although the analytical results obtained from the single-fibre model are close to those from experiments [14], the relations between the effective properties and the microstructure cannot be well explored with this model. In Ref. [9] the interaction of fibres under thermal loading was studied. It was pointed out that the single-fibre model may be inaccurate because the stress near the fibre depends strongly on the distance between the fibres. It has also been shown in Ref. [10] that non-uniform distribution of fibres significantly affects the local thermal residual stresses, but has little effect on the effective thermal coefficient of expansion. The effect of some typical non-uniform distributions of continuous fibres on the effective Young's modulus of composites has been studied in Ref. [15] with reference to local elasto-plastic stress fields. In Ref. [16] the fibre-cluster problem of unidirectional short fibre composites was treated. It was pointed out that the distribution of fibres significantly affects the local stress fields and the tangent modulus in the range of elasto-plastic deformation. However, the effect of bundling or contact of fibres on the effective transverse mechanical properties of fibre composites has not yet been investigated. This is the motivation of this work.

2.2. Fibre bundling model

Since the single-fibre model has the drawbacks discussed above, the fibre bundling model, which takes account of the interaction between fibres, seems to be more efficient in modelling certain fibre composites. Multi-fibre fragmentation tests have been developed to illustrate the effect of fibre interaction on the mechanical properties of composites [17]. The Micro-Raman spectrum is also used to investigate the interaction between fibres [18].

It should be noted that the main mechanical feature of fibre-bundle reinforced composites is the interaction and contact between fibres, which significantly influence the effective properties of the composites. One explanation is that the effective fibre radius has been increased. This also enhances the shielding effect of fibre bridging on matrix cracks and improves the fracture resistance of composites [12]. Moreover, the bundling of fibres changes the interfacial structure of fibre–matrix and can affect the growth orientation of cracks.

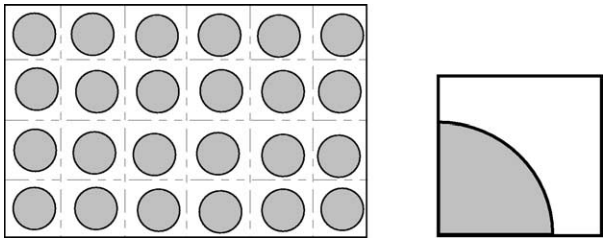

Fig. 2. Composite reinforced by uniform single fibres (Case 1). (a) Uniform reinforcement; (b) unit cell.

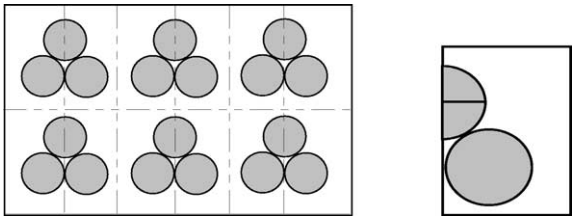

Fig. 3. Composite reinforced by three-fibre bundles (Case 2). (a) Uniform arrangement; (b) unit cell.

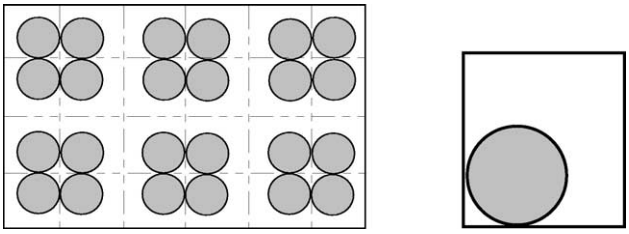

Fig. 4. Composite reinforced by four-fibre bundles (Case 3). (a) Uniform arrangement; (b) unit cell.

The interaction and contact between fibres can be best studied by using fibre bundling micromechanics models (Figs. 3 and 4). Since the main purpose of this work is to explore the basic properties of fibre bundling micromechanics models, three- and four-fibre bundle reinforced composite models are only considered here for illustration. Models with other fibre numbers such as two-, five-fibre bundles, can be treated similarly. The representative volume cells for three- and four-fibre bundles are shown in Fig. 3 and Fig. 4.

3. Finite element analysis

The typical finite element meshes for the three cases mentioned above (Figs. 2–4) utilized in the present analysis are shown in Fig. 5, where constant strain triangle elements are used. Point contact between the fibres in a bundle is assumed in the analysis, i.e. the fibres within a bundle contact each other at a point where no bond exists. The displacements across the interface are assumed to be continuous except at the contact point of fibres.

In the finite element analysis, it is assumed that the fibre is linearly elastic and its stress–strain relation obeys Hook's law, while the matrix material is assumed to be isotropic elasto-plastic. It is described by path-independent J_2 deformation theory with piecewise power hardening. In uniaxial tension, the material deforms according to

$$\frac{\sigma}{\sigma_0} = \begin{cases} \varepsilon/\varepsilon_0 & \varepsilon < \varepsilon_0 \\ (\varepsilon/\varepsilon_0)^n & \varepsilon \geqslant \varepsilon_0 \end{cases} \tag{1}$$

where σ_0 is the initial yield stress, $\varepsilon_0 = \sigma_0/E$ the yield strain, E the elastic modulus and $n (0 \leqslant n \leqslant 1)$ the strain hardening exponent. A perfect plastic matrix corresponds to $n = 0$. An elastic matrix material pertains

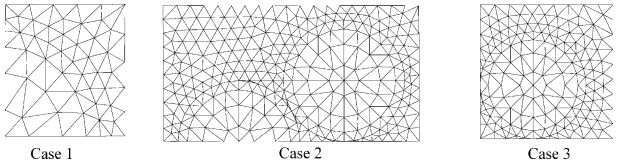

Fig. 5. Typical finite element meshes.

when $n = 1$. Under multiaxial stress states, the strain is written as the sum of an elastic part, ε_{ij}^{e}, and a plastic part, ε_{ij}^{p} :

$$\varepsilon_{ij} = \varepsilon_{ij}^{e} + \varepsilon_{ij}^{p} \tag{2}$$

$$\varepsilon_{ij}^{e} = \frac{1+v}{E} s_{ij} + \frac{1-2v}{3E} \sigma_{kk} \delta_{ij} \tag{3}$$

$$\varepsilon_{ij}^{p} = \frac{3}{2} \left(\frac{1}{E_s} - \frac{1}{E} \right) s_{ij} \tag{4}$$

Here v is Poisson's ratio, and E_s is the ratio of stress and strain in uniaxial tension, $s_{ij} = \sigma_{ij} - \frac{1}{3}\sigma_{kk}\delta_{ij}$ is the stress deviator.

Combining Eq. (3) and Eq. (4) gives

$$s_{ij} = \frac{E_s}{1+v_s} e_{ij} \tag{5}$$

$$\sigma_{kk} = \frac{E}{1-2v} \varepsilon_{kk} \tag{6}$$

where $e_{ij} = \varepsilon_{ij} - \frac{1}{3}\varepsilon_{kk}\delta_{ij}$ is the strain deviator, and v_s is the effective Poisson's ratio given by

$$v_s = \frac{1}{2} + \frac{E_s}{E} \left(v - \frac{1}{2} \right) \tag{7}$$

The solution to the non-linear finite element is obtained by a modified Newton–Raphson method which is second-order convergent [19].

4. Numerical assessment and discussion

In this section, the numerical results for stress–strain relationship attributable to the distribution of fibre bundles are presented to illustrate the effect of fibre bundles on the effective elasto-plastic properties of fibre composites. For simplicity, we consider only the problem of boron/aluminium composite material subjected to transverse tension or shear loads. The elasto-plastic stress–strain curves are predicted numerically for each loading case. The material constants are given by:

- Boron: Young's modulus $E_1 = 400$ GPa, Poisson's ratio $v_1 = 0.23$
- Aluminium: Young's modulus $E_0 = 68.9$ GPa, Poisson's ratio $v_0 = 0.35$, initial yield stress $\sigma_0 = 68.9$ MPa, strain hardening power $n = 0$, 0.2 and 0.5.

In all calculations, the volume fraction of fibre bundles is taken as $c = 0.5$.

4.1. Transverse tension loading

When subjected to transverse tension load, the boundary conditions of the unit cell (Figs. 2–4) can be expressed as

$$x = 0: \quad u = 0, \qquad x = a: \quad u = \bar{u}$$

$$y = 0: \quad v = 0, \qquad y = b: \quad v = \bar{v} \tag{8}$$

Note that a and b represent the length of the cell along x and y axes, respectively. Here $\bar{u}$ is the known applied displacement, while $\bar{v}$ may be determined from the condition of compatibility between the neighbouring cells. The compatibility of the null average normal stress on the boundary, $y = b$, is used in this study.

Fig. 6, Fig. 7 and Fig. 8 show the average stress–strain curves for the three cases, i.e. Cases 1, 2 and 3, respectively. Three different hardening exponents ($n = 0$, 0.2, 0.5) for the matrix are considered for each case.

The effect of fibre bundling on the overall properties of composites becomes apparent when comparing the overall properties of the single-fibre and fibre-bundle composites. In particular, fibre bundling can change the transverse isotropy of composites. For example, four-fibre bundle composite has different properties for angles of 0° and 45° in the transverse plane. The stress–strain relation in the direction of 0° (or 90°) is considered here.

For comparison, the numerical results are rearranged such that the average stresses for the three cases of fibre-bundle models are combined in one figure. Fig. 9, Fig. 10 and Fig. 11 show the results of fibre composites for $n = 0$, 0.2 and 0.5, respectively. It can be seen from these figures that fibre bundling does not affect the elastic properties. However, there is a remarkable influence on the plastic deformation and tangent modulus for different strain hardening exponents. This influence decreases along with increases in the strain hardening exponent of the matrix. This indicates that the effect of fibre bundling on the elastic properties of composite materials decreases rapidly when n approaches unity.

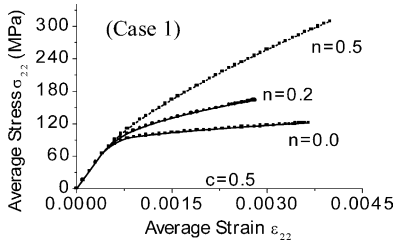

Fig. 6. Transverse normal stress–strain curves of single-fibre composites (Case 1).

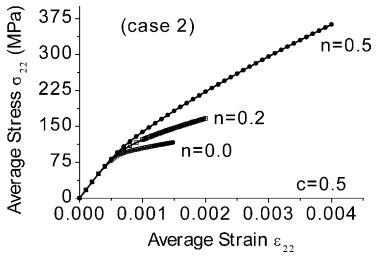

Fig. 7. Transverse normal stress–strain curves of three-fibre bundle composites (Case 2).

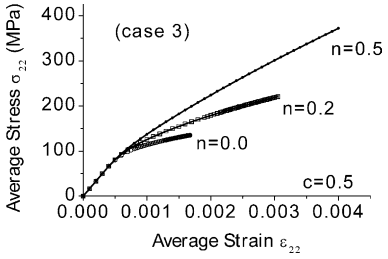

Fig. 8. Transverse normal stress–strain curves of four-fibre bundle composites (Case 3).

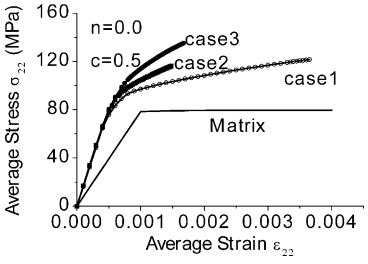

Fig. 9. Influence of fibre bundling on the transverse normal stress–strain curves ($n = 0$).

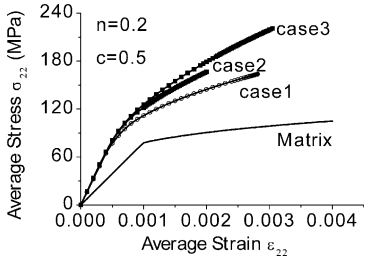

Fig. 10. Influence of fibre bundling on the transverse normal stress–strain curves ($n = 0.2$).

4.2. Transverse shear loading

The pure shear boundary conditions of the unit cell can be expressed as:

$$x = 0: \quad v = 0 \qquad x = a: \quad v = \bar{v}$$

$$y = 0: \quad u = 0 \qquad y = b: \quad u = \bar{u} \tag{9}$$

The finite element results for the transverse shear

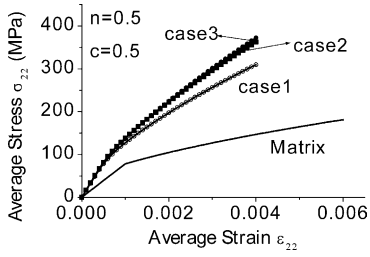

Fig. 11. Influence of fibre bundling on the transverse normal stress–strain curves ($n = 0.5$).

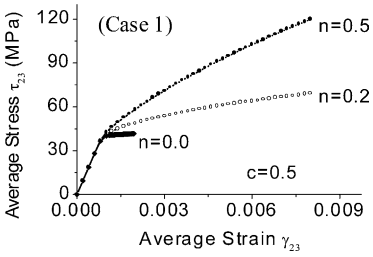

Fig. 12. Transverse shear stress–strain curves of single-fibre composites (Case 1).

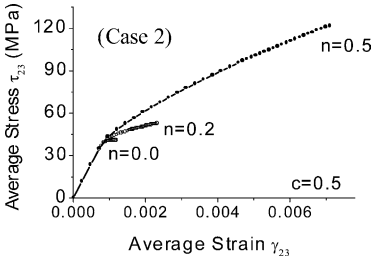

Fig. 13. Transverse shear stress–strain curves of three-fibre bundle composites (Case 2).

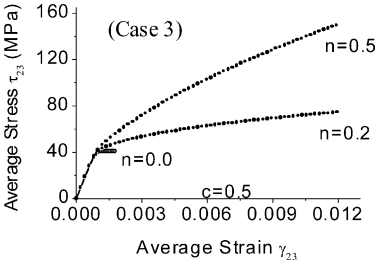

Fig. 14. Transverse shear stress–strain curves of four-fibre bundle composites (Case 3).

stress–strain relations of the three cases shown in Fig. 5 are given in Fig. 12, Fig. 13 and Fig. 14. It can be seen from the figures that the curves for each case are of the same shape. This indicates that type of fibre bundle has little effect on the mechanical properties of fibre composites. In contrast to the constitutive curves for matrix material, the curves for fibre-bundle reinforced composites are more precipitous and their elastic limits

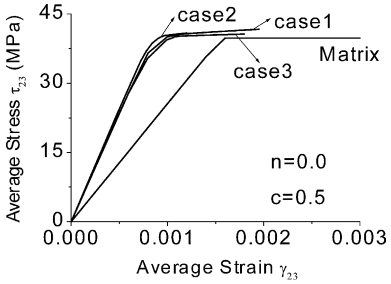

Fig. 15. Influence of fibre bundling on the transverse shear stress–strain curves ($n = 0$).

are much lower than for matrix. This indicates that a strong non-linear response of the material has been demonstrated earlier than in the matrix, which increases the ability of the composites to resist shear loading.

Fig. 15 shows the stress–strain curves for a perfect plastic matrix ($n = 0.0$). It can be seen from Fig. 15 that the average stresses, at any given value of strain except for the zero point, are all higher than that for the matrix. However, there is little discrepancy among the curves for the three types of fibre-bundle composites. This indicates that the material will be stiffer because of the presence of fibres, and the form of fibre bundle has negligible effect on the material properties when the matrix is perfect plastic.

The discrepancy in the average stress, at a given value of strain, between matrix and any one type of fibre-bundle composite become more apparent when n increases, which can be seen from Fig. 16 and Fig. 17. These results are very close to those of tensile cases, for the reason that there is a fixed quotient between stress obtained from shear loading and stress obtained from tensile cases (all parameters are the same). It can also be observed that the curves for Case 2 are the most precipitous of all the curves. The curves for Cases 1 and 3 are relatively consistent from the early stage of deformation and there is no apparent variation among curves of the two cases. This means that the fibre bundle in Case 2 has a greater effect on material properties than the other fibre bundles, while the fibre bundles of Cases 1 and 3 have a similar effect on the material properties of composites when subject to shear loading.

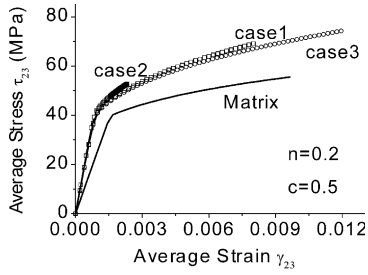

Fig. 16. Influence of fibre bundling on the transverse shear stress–strain curves ($n = 0.2$).

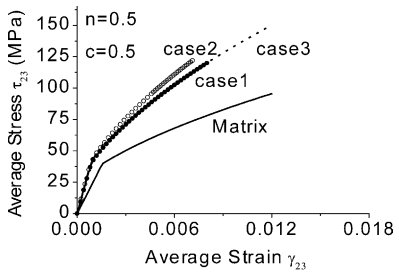

Fig. 17. Influence of fibre bundling on the transverse shear stress–strain curves ($n = 0.5$).

Fig. 15, Fig. 16 and Fig. 17 also show that the maximum stress and maximum strain for Case 3 are always greater than those of the other cases. To explain this, let us study Fig. 2, Fig. 3 and Fig. 4, the microstructures of each case. For Cases 1 and 3 the unit cell of the microstructure has bi-directional symmetry. Therefore one quarter of the unit cell can be used to simplify the calculating process. However, for Case 2 the unit cell has one symmetric plane, so only half the unit cell is available for simplifying calculation. Because microstructure is decided by the array form of fibres in the matrix, it can be concluded that the array of fibre bundles does have an effect on the properties of composite material under shear loading. In Case 2, a more irregular array occurs, and there is thus a stronger response against shear loading. This explains why the curves of Case 2 are shorter and more precipitous than those of Cases 1 and 3, as shown in Fig. 9, Fig. 10 and Fig. 11. Also, a higher local distribution density of fibre bundles among the matrix in Case 3 explains why the maxima of stress and strain in this case are relatively greater.

It should be pointed out that the above calculated results show trends only and may not represent the corresponding curves of real B/Al composites as the effects due to residual stresses in the constituents and weak fibre–matrix bonds have been neglected in the calculation.

5. Conclusions

The transverse normal and shear elasto-plastic stress–strain curves of fibre-bundle composites have been presented. These curves show that the main mechanical behaviour of fibre-bundle composites is attributable to fibre interaction. It is shown that there is a remarkable influence of fibre bundling on plastic deformation, transverse tension and shear tangent stiffness of composites, while the influence on effective elastic properties can be ignored. Further conclusions of this study can be summarized as follows:

(1) The effect of fibre bundling on transverse elastic stiffness constants can be ignored. This conclusion has been known previously and justifies the use of the single-fibre model for estimating the elastic modulus of composites, both in longitudinal and transverse directions.

(2) Fibre bundling enhances the transverse tangent stiffness of plastic deformation of composite materials. This effect depends on many factors, such as the strain hardening exponent of the matrix, arrangement geometry of fibre bundles, etc.

(3) The influence of fibre bundling on the effective stress–strain curves of composites increases as the deformation increases.

(4) The transverse normal stress–strain relations are more sensitive to fibre bundling than the transverse shear stress–strain relations.

References

[1] M.R. Piggot, Adv. Comp. Mater. 6 (1) (1996) 75–79.
[2] R. Paar, J.L. Valles, R. Danzer, Mater. Sci. Eng. A 250 (1998) 209–216.
[3] L. Ye, K. Friendrich, J. Mater. Processing Tech. 48 (1995) 317–324.
[4] C. Rospars, E. Le Dantec, F. Lecuyer, Composites Sci. Tech. 60 (2000) 1095–1102.
[5] R. Marissen, L.Th. Drift, J. Sterk, Composites Sci. Tech. 60 (2000) 2029–2034.
[6] M.F. Fu, J. Saczuk, H. Stumpf, Int. J. Eng. Sci. 36 (1998) 1741–1762.
[7] Y. Wang, Y. Xia, Composites Sci. Tech. 60 (2000) 591–596.
[8] A. Domnanovich, H. Peterlik, K. Kromp, Composites Sci. Tech. 56 (1996) 1017–1029.
[9] D. Kouris, E. Tsuchida, Mech. Mater. 12 (1991) 131–146.
[10] B.F. Sorensen, R. Talreja, Mech. Mater. 16 (1993) 351–363.
[11] M. Fila, C. Bredin, M.R. Piggott, J. Mater. Sci. 7 (1972) 983–988.
[12] J.-K. Kim, Y.-W. Mai, Comp. Sci. Tech. 49 (1993) 51–64.
[13] M.R. Piggott, Recent work on mesostructures and the mechanics of fiber composites, in: R. Pyrz (Ed.), IUTAM Symposium on microstructure-property interactions in comp maters, KAP, The Netherlands, 1995, pp. 375–385.
[14] H. Tolonen, S.G. Sjolind, Mech. Composite Mater. 31 (1995) 435–445.
[15] H.J. Bohm, Fiber arrangement effect on the microscale stresses of continuously reinforced MMCS, in: R. Pyrz (Ed.), IUTAM Symposium on microstructure-property interaction in comp maters, KAP, The Netherlands, 1995, pp. 50–61.
[16] Q. Yang, L. Tang, H. Chen, Acta Materiae Compositea Sinica 12 (3) (1995) 76–82.
[17] Z.F. Li, Comp. Sci. Tech. 54 (1995) 251–272.
[18] L.S. Schadler, et al., Mech. Mater. 23 (1996) 205–216.
[19] M. Ortiz, E.P. Popov, Int. J. Numer. Meth. Eng. 21 (1985) 1561–1576.